Top Med Chem (2019) 32: 111–132
DOI: 10.1007/7355_2018_44

Published online: 23 June 2019

Discovery of Elbasvir

Craig Coburn

Contents

Abstract On January 28, 2016, the US Food and Drug Administration approved Zepatier™ (a fixed-dose two-drug combination containing the NS5A inhibitor elbasvir and the NS3/4A protease inhibitor grazoprevir) for the treatment of adult patients with chronic hepatitis C virus genotype 1 or genotype 4 infection. The discovery of elbasvir (EBR) was the result of a concerted research effort within Merck's newly formed External Basic Research (also, EBR) group and a team of scientists from WuXi AppTec. Lead ID efforts combined components from both internal and literature compounds to generate a first-generation benzofuran-based NS5A inhibitor (MK-4882) that demonstrated preclinical proof of concept before entering phase 1 clinical trials. Lead optimization efforts and refinement of the core structure ultimately led to the identification of elbasvir, a ring-constrained tetracyclic indole-based analogue of MK-4882 which showed increased potency against clinical resistance variants and an improved resistance profile.

C. Coburn (✉)
Gossamer Bio, San Diego, CA, USA
e-mail: ccoburn@gossamerbio.com

Keywords EBR, Elbasvir, External research, HCV, MK-4882, MK-8742, NS5A inhibitor, Zepatier

1 Background

A series of breakthrough cures for hepatitis C began earning approval from the US FDA in 2014 of which inhibitors targeting the viral nonstructural protein 5A (NS5A) emerged as a key component of the direct-acting antiviral (DAA) regimens. As of March 2018, these included daclatasvir, ombitasvir, ledipasvir, elbasvir, pibrentasvir, and velpatasvir – each of which shows remarkable potency against a wide variety of genotypes and resistance mutations. Combination of these agents with other DAAs has demonstrated sustained virologic response rates >90% after only 8–12 weeks of therapy.

NS5A inhibitors were originally identified by phenotypic screening campaigns using HCV sub-genomic replicons, and these efforts produced a number of structural chemotypes that displayed low nanomolar EC_{50} values against genotype 1b but weaker activity against other genotypes. Pioneering work by the BMS team on a series of symmetric bis-pyrrolidines catalyzed discovery programs across pharma with a seminal report in 2010 that showed clinical validation of a highly potent and pan genotypic inhibitor of HCV NS5A [1]. Structural features of this compound can be found in each of the six currently marketed NS5A inhibitors.

For nearly 30 years, HCV discovery research teams at Merck pursued multiple molecular targets in the search of a cure. The NS5A project took root at its IRBM site where the team discovered a series of piperazine-based small molecules that inhibited HCV replication but did not show activity in any of the typical HCV enzyme assays. The partial mode of action was subsequently characterized and linked to their ability to alter NS5A biogenesis which resulted in a reduction of p56–p58 conversion, and the resistance mutations identified were mapped to NS5A [2].

Early in 2008 the NS5A project was transferred to the newly formed External Basic Research (EBR) group whose chemistry team was headed by Joseph Vacca and then later by Peter Meinke. EBR was comprised of a small group of senior medicinal chemistry leaders from several sites across the Merck network whose mandate was to carry out medicinal chemistry projects using ex-US resources for all early discovery activities including synthetic chemistry, assay screening, and routine PK-ADME work.

I assumed leadership of the HCV NS5A project (called EBR-8) and initiated lead identification work with a team of 25 chemists from WuXi AppTec who were based in Shanghai, China. Chemists on the team were, at first, inexperienced in drug discovery but extremely productive and eager to learn medicinal chemistry concepts in order to participate in SAR development and target generation. All project data was shared in real time, and weekly teleconferences and regular site visits formed the basis of a cohesive team. The WuXi EBR-8 chemistry team under the local

leadership of Hao Wu, Bin Hu, Bin Zhong, and Richard Soll would become instrumental in the discovery of elbasvir (ironically abbreviated as EBR).

2 Lead Identification

With the IRBM compounds as a starting point, initial efforts focused on the synthesis and SAR development of these *N*-arylpiperazines (**1**) (Fig. 1). The incorporation of a cyclic constraint within these structures afforded indole **2**, which showed similar potency in the replicon assay (GT1b EC_{50} ~150 nM) and was an attractive entry toward modulating this target. Concurrent to these efforts, other NS5A inhibitors began to appear in the patent literature, but their SAR had not been fully delineated. Because of the structural similarity between compound **1** and the stilbene inhibitors **3** [3], a lead-hopping effort was initiated with the goal of applying a similar cyclization strategy in order to explore the SAR of the pseudosymmetric isosteres **4**. Subsequent reports revealed that compound **3** was also pivotal in the design of daclatasvir [4, 5].

Several heterocyclic scaffolds (**4a–4f**) (Table 1) were synthesized and incorporated into the final inhibitor structures. The cellular activity of each new compound was determined using the replicon-system-expressing genotypes 1b, 2a, and 1a. Initial results showed that benzimidazole **4a**, benzothiazole **4b**, and benzoxazole **4c** each had in vitro profiles worse than the parent stilbene inhibitor **3**, whereas

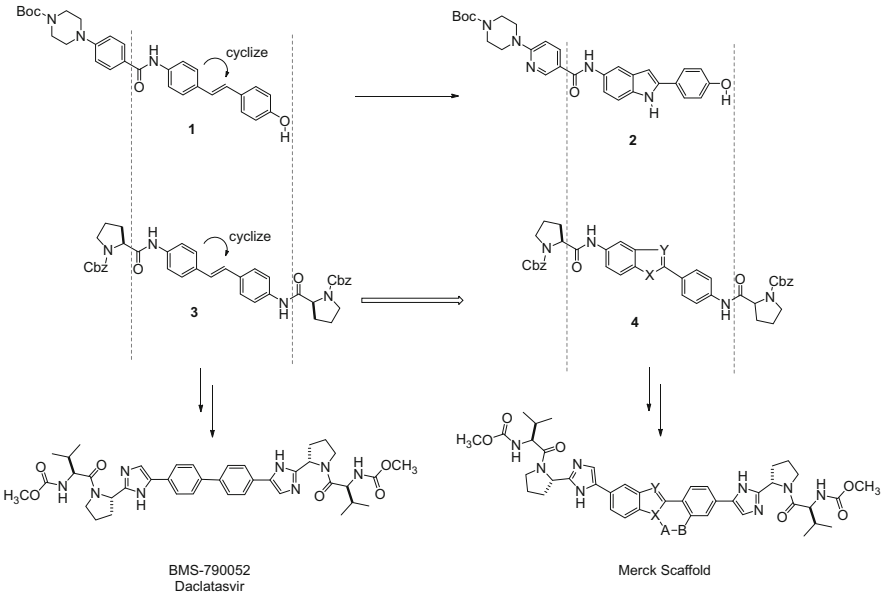

Fig. 1 Strategy for the development of NS5A inhibitors

Table 1 Central scaffold SAR

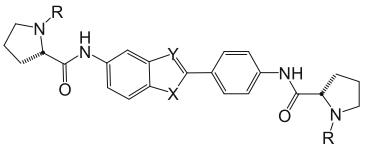

Compound	Substituent		Genotype, EC_{50} (nM)		
	R	X, Y	1b	2a	1a
3			5	60	>20,000
4a	Cbz	NH, N	>20,000	>20,000	>20,000
4b	Cbz	S, N	>20,000	>20,000	>20,000
4c	Cbz	O, N	160	1,500	>20,000
4d	Cbz	O, CH	5	230	>20,000
4e	Cbz	NH, CH	16	290	1,600
4f	Cbz	NCH_3, CH	170	990	>20,000
4g	Cbz	CH, NH	>20,000	>20,000	>20,000
5	$PhCH_2CH_2$	NH, CH	4	290	2,100
6	(*S*)-Boc-Phe	NH, CH	14	nd	nd
7	(*S*)-Boc-Phg	NH, CH	0.4	20	1,500
8	(*R*)-Boc-Phg	NH, CH	0.004	0.05	70

benzofuran **4d** and indole **4e** had profiles similar to the reference compound. Alkylation of the indole nitrogen atom resulted in an ~tenfold loss in replicon activities (**4f**), whereas the isomeric 2,6-disubstituted indole **4g** resulted in a substantial loss in potency relative to **4e**. Within the context of the indole-based scaffold, replacement of the proline *N*-Cbz group by either the isosteric hydrocinnamate ligand (**5**) or an (*S*)-*N*-Boc-phenylalanine group (**6**) did not have a significant influence on potency. Synthesis and evaluation of the (*S*)-*N*-Boc-phenylglycine (Phg) homolog **7** showed a tenfold increase in genotype 1b and 2a potencies, while the epimeric (*R*)-*N*-Boc-Phg-containing diastereomer **8** afforded a 100- to 400-fold increase in GT1b and GT2a potencies and a 20-fold improvement in GT1a potency (Table 1).

Additional profiling of inhibitor **8** showed bioavailability to be low (<2%) in preclinical animal models with poor oral absorption attributable to the high peptidic nature of the compound. To address this limitation, the C2'-phenyl amide bond was replaced by a variety of amide isosteres (Fig. 2; Y = NH).

These modifications, however, resulted in compounds that displayed inferior replicon profiles relative to the parent amide **8**. Pyrazole analogue **11** appeared to have the best profile, and it was speculated that the NH group was important for maintaining genotype 1a and 1b potencies. As such, imidazole **13** was synthesized, and whereas EC_{50} values versus GT1b and 2a were similar to those of amide **8**, this modification resulted in an ~20-fold improvement in genotype 1a potency (EC_{50} = 3 nM). Further exploration into the SAR of NH-containing heterocyclic amide isosteres resulted in the synthesis of the isomeric 2-prolyl-5-phenylimidazole analogue **14**. This modification gave an additional ~20-fold increase in potency

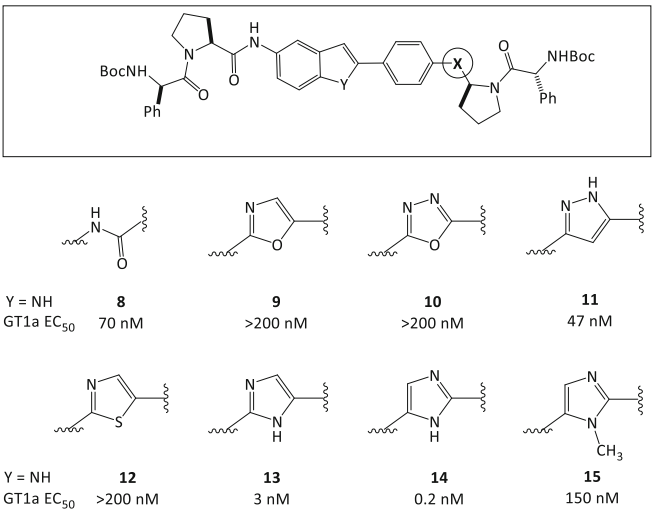

Fig. 2 Amide isosteres and genotype 1a potency

Table 2 Imidazole SAR

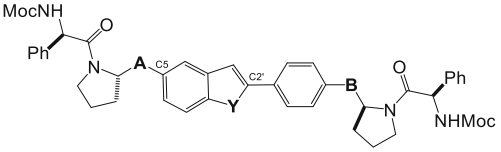

	Substituent		Genotype, EC_{50} (nM)[a]			C_{max}[b]
Compound (Y = O)	A	B	1b	2a	**1a**	uM
16	Amide	Amide	0.01	0.01	**27**	0.03
17	Imidazole	Amide	0.002	0.004	**2**	0.01
18	Amide	Imidazole	0.006	0.002	**0.3**	0.03
19	Imidazole	Imidazole	0.004	0.004	**0.015**	0.02

[a] $n = 3$
[b] 10 mpk PO dosed in 10% Tween to fasted male SD rats

against GT1a while maintaining low-picomolar EC_{50} values in the GT1b and GT2a replicon assays. The importance of the heterocyclic NH substituent was further proven by the loss in replicon potency of the *N*-methylated analogue **15**. Altogether, the incorporation of the imidazole amide isostere maintained both GT1b and 2a potency while improving GT1a potency by ~400-fold relative to the amide **8**.

3 Lead Optimization

Both single and double imidazole amide isosteres in the benzofuran series (Table 2; Y = O) were prepared to further explore the effects of the 2-prolyl-5-arylimidazole substitution on both potency and pharmacokinetics. Table 2 shows the results from imidazole incorporation first on the C5 benzofuran side (**17**; A = imidazole) and then the C2' phenyl side (**18**; B = imidazole). In each case, genotype 1b and 2a potencies remained the same, while genotype 1a potency improved by a factor of 10. Incorporation of both imidazole amide isosteres (**19**; A = B = imidazole) resulted in an additional 20-fold improvement in GT1a EC_{50} values. On the basis of the low-picomolar EC_{50} values in GT1a, 1b, and 2a replicon assays, compound **19** became an important lead. Subsequent research efforts focused on the SAR of the terminal amino acid groups in order to address the problematic oral absorption profile without perturbing the virologic profile. Table 3 shows the area under the curve values after 10 mg/kg oral dosing to fasted male Sprague–Dawley rats for some of the amino acids surveyed. With the exception of compound **21**, little difference in GT1a potency was observed upon incorporation of various alkyl and cycloalkyl substituents.

Conversely, plasma drug exposure depended heavily on the nature of the amino acid substituent. For example, replacement of the C2' phenyl side D-phenylglycine residue with an L-valine subunit (**20**; Y = (*S*)-^{i}Pr) resulted in 20-fold higher compound exposure than analogue **19** (Y = (*R*)-Ph). The addition of a second L-valine group (X = (*S*)-^{i}Pr) **21** resulted in even higher plasma drug levels after 10 mg/kg oral dosing. Additionally, compound **22**, which has an *S,S,S,S* configuration, showed 420-fold higher plasma AUC values than its *R,S,S,S* diastereomer **21**. Further SAR on a variety of homologated valine analogues (i.e., cyclopropyl glycine **23**, tert-butyl glycine **24**, isoleucine **25**, homoalanine **26**) showed better exposure than **19**, although each was inferior to **22**. Cyclopropyl glycine analogue **23** displayed similar plasma drug exposure and oral bioavailability in the rat while maintaining good potency in the GT1a and GT1b replicon assays. However,

Table 3 Amino acid SAR

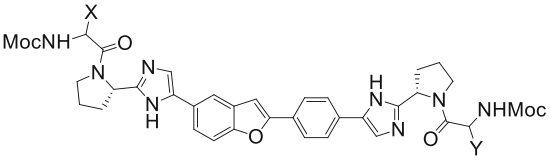

Cmpd	X	Y	AUC (uM*h)
19	*R*-phenyl	*R*-phenyl	0.5
20	*R*-phenyl	*S*-isopropyl	10
21	*R*-isopropyl	*S*-isopropyl	0.1
22	*S*-isopropyl	*S*-isopropyl	42
23	*S*-cyclopropyl	*S*-cyclopropyl	38
24	*S*-tert-butyl	*S*-tert-butyl	10
25	*S*-sec-butyl	*S*-sec-butyl	2
26	*S*-ethyl	*S*-ethyl	7

Table 4 Profiles of compound **22** (MK-4882) and **23**

	Genotype, EC_{50} (nM)				10 mpk PO rat	
Cmpd	1b	2a	1a	1aY93H	AUC (uM*h)	%F
22	0.001	0.05	0.01	27	42	38
23	0.003	6.2	0.07	230	38	45

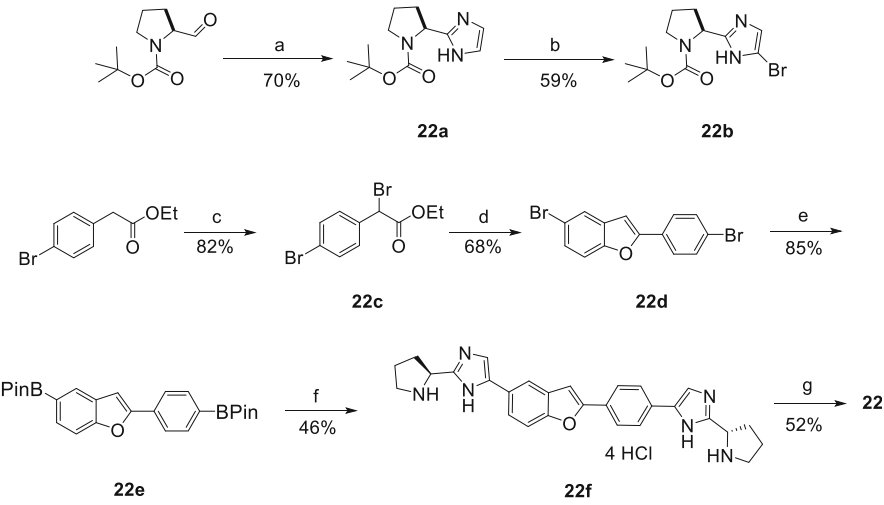

Scheme 1 Synthesis of MK-4882. (**a**) Glyoxal. 7N NH_3 in MeOH. (**b**) i. NBS, THF; ii. Na_2SO_3, EtOH, water, reflux. (**c**) NBS, HBr, CCl_4. (**d**) 5-Bromosalicylaldehyde, Cs_2CO_3, DMF, reflux. (**e**) Bis(pinacolato)diboron, KOAc, Pd(dppf)Cl_2, dioxane, reflux. (**f**) i. **22b**, Na_2CO_3, Pd(dppf)Cl_2, THF, water, reflux; ii. HCl, MeOH. (**g**) *N*-Moc-L-valine, BOP, DIPEA, DMF

examination of the overall potency profiles of **22** versus **23** showed a significant loss in potency against both GT2a and the key genotype 1a Y93H mutants. As such, compound **22** was selected for early clinical development as MK-4882 (Table 4).

The synthesis of MK-4882 is straightforward and is illustrated in Scheme 1. *N*-Boc-L-proline aldehyde was converted into the 2-substituted imidazole **22a** using a Radziszewski imidazole synthesis in good yield. Imidazole **22a** was subsequently treated with excess NBS in THF to give the C4,C5-dibrominated intermediate, which was reduced with sodium sulfite to provide the key mono-brominated imidazole intermediate **22b**. The 2-phenylbenzofuran scaffold was easily prepared via one-pot Cs_2CO_3-mediated alkylation/intramolecular cyclocondensation between 5-bromosalicylaldehyde and ethyl-2-bromo-(4-bromophenyl)acetate (**22c**). Metal–halogen exchange of 5-bromo-2-(4-bromophenyl)benzofuran (**22d**) afforded the bis-pinacol boronate ester, which was subsequently coupled to bromoimidazole **22b**. Deprotection of the proline Boc groups afforded penultimate compound **22f**, which was subjected to an amide coupling protocol using the BOP reagent and two equivalents of *N*-methoxycarbonyl-L-valine.

MK-4882 was found to be highly potent against both genotypes 1a and 1b, with EC_{50} values in the low-picomolar range, and showed only a three- to fourfold shift in

the presence of 40% normal human serum. A number of clinical, in vivo, and in vitro studies have identified key mutations that confer resistance to NS5A inhibitors [6, 7]. These mutations arise principally at residues 28 (1a and 1b), 30 (GT1a), 31 (GT1a and GT1b), and 93 (GT1a and GT1b). MK-4882 potency is shifted to low nanomolar against many mutations at the key NS5A residues 30, 31, and 93. Typically, the magnitude of the potency shift was greater in the GT1a background. For example, MK-4882 potencies against L31V and Y93H mutants in the GT1b background were 0.5 and 3.0 nM, respectively, whereas in the genotype 1a background, they were 2 and 27 nM. Data are summarized in Table 5.

The pharmacokinetic properties of MK-4882 were studied in Sprague–Dawley rats, beagle dogs, and rhesus monkeys. MK-4882 demonstrated low clearance and moderate half-life (2–5 h) in the three species. The oral bioavailability was 26% in dog and 38% in rat, demonstrating that the compound was moderately absorbed in preclinical species. The T_{max} in both rat and dog was somewhat long at 4–6 h. MK-4882 demonstrated slightly greater than dose-proportional exposures in rat when dosed at 2 and 100 mpk and also in dog between oral doses of 1 and 50 mg/kg. Unlike many of the HCV protease inhibitors, MK-4882 did not appear to undergo transport-mediated uptake into the liver, as the liver-to-plasma ratio averaged <10 after oral dosing to rats. The oral absorption profile in chimpanzees was also evaluated in preparation for in vivo efficacy studies. As such, two male chimpanzees were dosed orally with MK-4882 at 1 mpk as a suspension in Tang, and both plasma and liver levels were determined. Twelve-hour average plasma and liver concentrations were 0.19 and 1.3 μM, respectively. Total free drug concentration in plasma at C_{24h} (~3 nM) was greater than the genotype 1b wild-type and genotype 1b mutant EC_{50} values (Table 6).

Table 5 MK-4882 in vitro potency profile vs. GT1 and key mutants

Genotype	EC_{50} (nM)	Genotype	EC_{50} (nM)
1a WT	0.01	**1b WT**	0.003
1a Q30H	5	**1b L28V**	0.03
1a Q30R	8	**1b R30Q**	0.001
1a L31F	2	**1b L31F**	0.17
1a L31V	6	**1b L31V**	0.5
1a Y93C	9	**1b Y93C**	0.02
1a Y93H	24	**1b Y93H**	2

Table 6 MK-4882 pharmacokinetics[a,b]

Species	Cl (mL/min/kg)	$T_{1/2}$ (h)	PO C_{max} (uM)	PO AUC (uM*h)	%F
Rat	9.3 ± 0.4	2.0 ± 0.1	0.31 ± 0.11	1.74 ± 0.27	38
Dog	6.4 ± 4.0	4.7 ± 0.5	0.19 ± 0.03	1.06 ± 0.06	26
Rhesus	9.1	3.0	0.18	1.44	12
Chimp	nd	nd	0.45	5.1	nd

[a]Rat, dog, and monkey iv (1 mg/kg, $n = 3$, 30% captisol + 2 equiv. HCl)
[b]Rat po (2 mg/kg, $n = 3$, 0.5% methylcellulose), dog po (1 mg/kg, $n = 3$, 0.5% methylcellulose), rhesus po (5 mg/kg, $n = 2$, 0.5% methylcellulose), and chimpanzee po (1 mg/kg, $n = 2$, Tang)

4 Pharmacological Activity

Both single-dose and multiple-dose studies in chimpanzees chronically infected with HCV were conducted to determine the antiviral efficacy of MK-4882. A single dose of MK-4882 was orally administered at 1 mpk as a suspension in Tang to three chronically infected chimpanzees. Two carried high viral load infections (~106 IU/mL) of GT1a or GT1b. The third had a GT1a viral load of 104 IU/mL that was homogeneous for the NS3 protease R155K mutation.

All three animals responded rapidly after the single dose; viral load was suppressed an average 2.15 log units within 12 h, with continued suppression to an average nadir of 2.91 log units at 48 h before rebounding. Initial 12 h viral load decreases were similar for both the GT1a and GT1b infections, but an additional one-log suppression was observed with the GT1b infection by 24 h. Suppression of the GT1a infection was maintained through this time but did not increase further. Plasma concentrations of MK-4882 in this study were similar to those found in the satellite study and ranged from 0.06 to 0.17 uM at 12 h, diminishing approximately by half at 24 h. Drug was cleared from plasma and was below the level of quantification (LOQ ~25 nM) by 48 h. The potency of the drug was sufficient to maintain viral suppression through at least 48 h. Drug concentration in the liver, as determined from liver biopsy samples, ranged between 0.77 and 1.56 μM at 12 h. The results are consistent with the satellite PK study in uninfected chimps. Resistance analysis was conducted by population sequencing of the NS5A gene of viral RNA isolated from serially collected plasma samples. The GT1b-infected chimp became homogeneous for the Y93H mutation after 24 h (sequence could not be generated for the 12 h time point, as no additional sample was available at this time). Viral load was further suppressed another 0.6 log units by 48 h, which suggests suppression of mutant virus. Early rebound virus at day 4 was also homogeneous for Y93H, but wild-type virus became the predominant population by day 7. An additional K44R polymorphism, co-encoded with the Y93H virus, was no longer observed at day 10 upon reemergence of wild-type virus, suggesting that mutant and wild-type viruses are two distinct populations. Sequencing of a sample collected on day 28 (4 weeks post-dose) showed the emergence of a new mixture of L31V/L virus. A similar late emergence of apparently distinct resistant virus was also observed in the GT1a (wild-type)-infected chimpanzee (see below). The reason for these phenomena is currently not understood, and the timing of the emergence of L31L/V virus cannot be further pinpointed, as plasma samples were not collected between days 10 and 28. Rebound virus from the GT1a (wild-type)-infected chimpanzee was heterogenous for both Q30E and Y93H. By day 7, Y93H was the only mutation detectable and as a mixed population with wild-type virus. By day 10 this evolved to a mixed population of Y93C and wild-type virus. The shift from Y93H to Y93C coincides with diminishing drug plasma levels and is consistent with the greater loss of potency observed with Y93H than Y93C in vitro. However, by day 28, virus evolved further to an L31M/V mixture. For both the GT1a and 1b infections, wild-type eventually re-emerged as the principle viral population (data

not shown). For the chimpanzee encoding the GT1a NS3 R155K infection, L31M/L was detected as a mixed population at day 10, and only wild-type virus was detected on day 28. Although MK-4882 exhibited a robust virologic response after a single 1 mpk dose, the emergence of mutant virus in the rebound phase warranted further evaluation of efficacy following multi-dose administration. Two different HCV-infected chimpanzees (GT1a and GT1b), both treatment-naïve to NS5A inhibitors, were dosed orally at 1 mpk once daily for 7 days. Liver biopsies were collected 12 h following the final dose; drug concentrations in the liver were 7–15-fold higher than plasma levels, consistent with the findings in the Sprague–Dawley study and suggested that MK-4882 was not selectively retained in liver tissue.

The results from the study showed a rapid and robust response immediately following the initial dose, with an average maximal decrease in viral load by ~3.5 log units. The GT1b-infected chimpanzee showed a further decline in viral titer through the duration of the study, reaching a maximal 3.8-log suppression of virus by day 7 before rebounding. Virus was mixed with Y93H/Y population at day 10 (3 days post-dosing) and eventually became homogeneous for wild type (data not shown). Although the initial response in the GT1a-infected chimpanzee was robust, viral breakthrough was noted beginning at day 2. This eventually led to a 2-log increase in viral titer during dosing, although viral load was still suppressed greater than 1 log from pre-dose levels. Sequence analysis showed that at day 6 virus collected from this animal was heterogenous for both Q30R and L31M/L. A similar viral mixture was observed at day 10 (3 days post-dosing). Eventually wild-type virus emerged as the principle population.

MK-4882 entered the clinic supported by an eCTA preclinical safety paradigm with a single rising dose study in healthy male volunteers in October 2010. MK-4882 was generally safe and well tolerated following single doses as high as 400 mg. The prespecified PK target ($C_{24hr} \geq 20$ nM) was reached at doses of MK-4882 higher than 25 mg, and the average half-life across all groups was 17.2 h.

At the same time, a 3-month oral toxicity study in dogs was initiated to support subsequent longer duration clinical dosing. The MK-4882 low-, mid-, and high-dose levels in this study were 10, 50, and 1,000 mg/kg/day. The high-dose group received 1,000 mg/kg/day for 2 weeks, with doses lowered sequentially to 500 mg/kg/day and then 200 mg/kg/day. The MK-4882 exposure in the low-dose group was 14 μM h which was seven times higher than the clinical efficacy target of 2 μM h. Exposure for the high-dose group was not proportional to the low-dose group (AUC = 71 μM h) due to limited absorption. Noteworthy in this study was the finding that one of six dogs in the high-dose group showed white-matter brain degeneration at necropsy which did not repeat in several follow-up studies. As a consequence of this toxicological finding, along with the viral breakthrough evidenced in the preclinical proof-of concept efficacy studies and the fact that more promising compounds were starting to emerge from the laboratories, MK-4882 were placed on hold in February of 2011.

5 Second-Generation Analogues of MK-4882

The viral breakthrough evidenced in the preclinical proof-of-concept efficacy studies for MK-4882 necessitated the design of newer NS5A inhibitors with improved safety and virologic profiles against the various genotypes and resistance mutations. SAR of the benzofuran core structure suggested that the introduction of a cyclic constraint could result in more potent inhibitors. The initial strategy involved linking the C3 benzofuran carbon to the C2' phenyl carbon to afford tetracyclic core structures **27** and **28** (cyclization mode a; Fig. 3).

Evaluation of these compounds in the replicon assay showed that these modifications resulted in a loss in potency versus the wild-type forms of GT1a and 1b as well as the key mutants L31V and Y93H. An alternative mode of cyclization (mode b) was examined and was made possible by converting the benzofuran core to an indole scaffold which allowed cyclization from the indole nitrogen to the phenyl C2' carbon through either an ethylene bridge (**29**) or an oxygen-containing bridge (**30–34**). These modifications afforded inhibitors that possessed a tetracyclic indole scaffold which proved to be equipotent to MK-4882 versus GT1a and GT1b wild-type replicon systems. Further evaluation showed that the GT1a Y93H potency was weakened with the carbon analogue **29** (EC_{50} = 170 nM) (Table 7). This activity was improved by incorporating an oxygen atom in the two-atom bridge of compound **30** (Y=O; GT1a Y93H EC_{50} = 5 nM). Noteworthy is the fact that the aminal linkage was extremely stable to hydrolytic cleavage even under forcing conditions. Despite having an improved virologic profile, the unique tetracyclic indole-containing compound **30** proved to be cytotoxic in the low-micromolar range (CC_{50} ~1 μM).

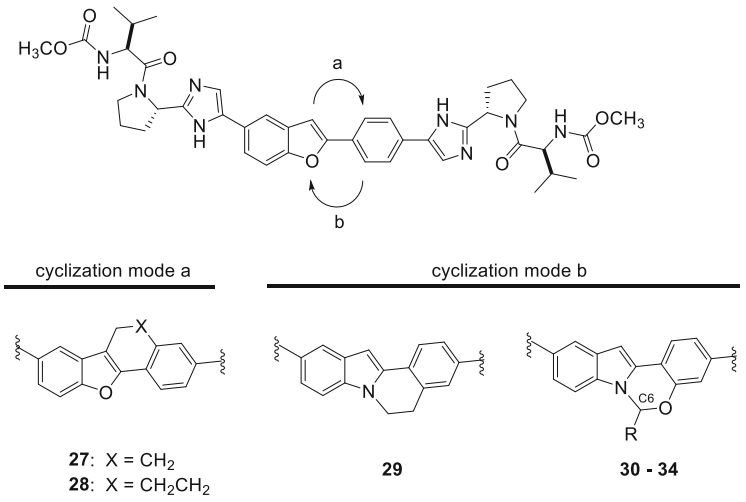

Fig. 3 Design strategy for second-generation NS5A inhibitors

Table 7 SAR for tetracyclic inhibitors

Cmpd	R	Genotype, EC_{50} (nM)					CC_{50} (uM)
		1b	2a	1a	1aL31V	1aY93H	
MK-4882	–	0.001	0.04	0.01	6	24	9
29	–	0.02	0.9	0.002	nd	170	1
30	H	0.001	0.16	0.002	2	5	1
31	CH_3	0.003	0.007	0.003	7	8	nd
32	CH_2CH_3	0.002	0.001	0.002	1	4	nd
33 (EBR)	S-Ph	0.003	0.003	0.004	0.5	2	>25
34	R-Ph	0.005	0.010	0.002	nd	60	>25

SAR analysis showed that the addition of an alkyl or aryl substituent at C6 could abrogate the cytotoxicity while maintaining a favorable potency profile. Initial studies focused on substituting the tetracyclic indole core with small alkyl groups (Table 7) [8]. The addition of a methyl group (**31**) showed good potency against genotypes 1a, 1b, 2a, and 3a, while the activity was weak on genotypes 2b (EC_{50} = 23 nM), 4a (EC_{50} = 0.03 nM), and 1a L31V (EC_{50} = 7 nM). An ethyl analogue (**32**) offered a potency profile similar to the methyl analogue with the exception of 10× better potency on GT2b (EC_{50} = 2 nM). Increasing the size of the alkyl group to *n*-propyl, *n*-butyl, or *n*-hexyl group did not result in improved potency and gave similar results as the ethyl analogue. The addition of fluorine atoms to the alkyl chain also had little effect on the virologic profile, while the introduction of either a terminal cyano group or an ester functional group reduced the potency against the GT1a Y93H mutant. The corresponding carboxylic acid analogue lost activity across all genotypes.

In addition to linear alkyl groups, a series of branched alkyl groups were incorporated into the tetracyclic scaffold at the C6 aminal carbon. The introduction of an isopropyl group resulted in a tenfold loss in GT2a and GT1a Y93H activity versus the corresponding ethyl analogue, while a cyclopropyl group improved the virologic profile in the replicon assay against genotypes 2b, 3a, and 1a Y93H. The potency profiles of cycloalkyl analogues of increasing ring size were also evaluated but proved to be >10× weaker against genotype 2b and several genotype 1a mutants.

Attention next turned to the incorporation of a variety of aryl and heteroaryl substituents for SAR evaluation. We began these SAR studies with the unsubstituted phenyl group and showed that the resulting mixture of diastereomers had a good potency profile. Chiral SFC separation of the two diastereomers afforded compound (**33**) and its diastereomer **34**. While the virologic profiles of the two diastereomers showed equivalent potency values in the wild-type replicons, compound **33** proved to be 25-fold more potent versus the GT1a Y93H mutant.

A series of six-membered heteroaromatic analogues were also synthesized and evaluated, but each of these compounds failed to show a better profile than the parental phenyl compound (**33**) [9]. Additionally, substitution of the C6 phenyl ring

generally resulted in poorer overall virologic profiles when compared to compound **34**. Notable exceptions were found with the *p*-*c*-propylphenyl and *p*-biphenyl analogues as well as the 3-alkoxyphenyl analogues which showed improved potency versus each of the genotypes and mutants assayed. Despite the improvements in potency, the pharmacokinetics of each of these analogues proved to be inferior to the unsubstituted phenyl compound; thus they were not advanced.

After extensive profiling, dimethyl *N,N′*-([(6*S*)-6-phenylindolo[1,2-c][1,3]benzoxazine3,10-diyl]bis{1*H*-imidazole-5,2-diyl-(2*S*)-pyrrolidine-2,1-diyl[(2*S*)-3-methyl-1-oxobutane-1,2-diyl]})dicarbamate (**33**), also known as L-002469825, MK-8742, Elbasvir, and EBR supplanted MK-4882 as Merck's lead clinical compound (Table 8). EBR was specifically described in US Provisional Patent Application No. 61/247,318, filed September 30, 2009, and PCT Application No. PCT/US2010/028653, filed March 25, 2010. The PCT application published on September 29, 2010, as International Publication No. WO 10/111,483. Both applications name inventors from Merck & Co., Inc. and WuXi AppTec Co., Ltd.

EBR was found to be highly potent against most HCV genotypes tested with EC_{50} values in the low-picomolar range and modest potency shifts in the presence of 40% NHS. EBR maintained significant potency against most of the NS5A mutations in the screening panel and showed (on average) an order of magnitude improvement relative to MK-4882. EBR potencies against the key L31V and Y93H mutants in the GT1b background were 0.01 and 0.05 nM, respectively, while in the genotype 1a background, they were 0.5 and 2 nM. EBR also demonstrated a favorable genotypic

Table 8 EBR in vitro potency profile GT1–4 and key GT1 mutants

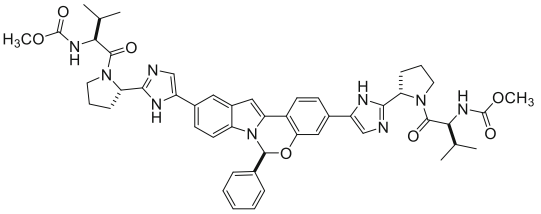

Genotype	EC_{50} (nM)	Genotype	EC_{50} (nM)
1a WT	0.004	**1b WT**	0.003
1a Q30H	0.03	**1b L28V**	0.004
1a Q30R	0.5	**1b R30Q**	0.009
1a L31F	0.08	**1b L31F**	0.05
1a L31V	0.5	**1b L31V**	0.01
1a Y93C	0.2	**1b Y93C**	0.005
1a Y93H	2	**1b Y93H**	0.05
1a Y93N	2	**2a (JFH) WT**	0.003
2a WT	0.003	**2b (JFH)**[a]	3
3a (con1)[a]	0.02	**4a(con1)**[a]	0.003

[a]Chimeric replicons with indicated NS5A patient sequences cloned into con1 or JFH background

virologic profile (Table 8). The decreased potency in the GT2b cell line is attributed to the presence of a methionine residue at position 31 of NS5A versus a leucine present in GT2a [10].

6 Pharmacokinetics and Metabolism Studies

The pharmacokinetics of EBR was studied in Wistar Han rats, beagle dogs, and cynomolgus monkey (Table 9). The i.v. clearance was moderate and constituted ~14–29% of hepatic blood flow in all three species. The V_{dss} was moderate, and the effective half-life was also moderate (2.5–5.9 h). The terminal half-life was longer (4–16 h) than the effective $T_{1/2}$, suggesting rate-limited return from tissue compartments. The oral bioavailability was low to moderate (9–35%) for all three species. The low to moderate bioavailability is likely due to limited absorption which is consistent with low passive permeability in MDCKII cells of 47 nM/s. Preclinical modeling of EBR suggested a high potential for low-dose once-daily dosing in the clinic.

EBR showed high plasma protein binding in all species (>99.9%). The compound was well distributed to the target organ (liver/plasma ratio in rats ~200×), while its uptake by the brain was low (brain/plasma ratio = 0.26). There was no indication of untoward accumulation or auto-induction upon multiple dosing in rats, with good exposure multiples obtained in dose limiting toxicity studies in the rat as well as in dog pharmacology study. In rats, the compound-derived radioactivity was excreted in urine, bile, and feces after IV administration with a significant percent of dose excreted in feces likely by secretion or efflux from the GI tract wall. Approximately 13% of the dose was excreted unchanged in urine, bile, and feces. Human PK and dose projection was carried out based on both allometry and IV/IVC which showed the effective half-life range of 10–14 h consistent with once-daily dose regimen with a dose range of ~50 mg, encompassing both loading and maintenance dose ranges. The compound was metabolized by hepatocytes of all species including humans to oxidative metabolites (M + 16 and M + 32) which were also the same metabolites observed in rats and dogs in vivo, with no glutathione or acyl glucuronide metabolites observed. There was no human-specific metabolite. EBR was found to be neither an inhibitor nor a potent inducer of major human CYPs; therefore potential DDI as a perpetrator with other CYP substrates was predicted to be low.

Table 9 Preclinical pharmacokinetics of elbasvir

Species	Cl (mL/min/kg)	$T_{1/2}$ (h)	PO C_{max} (uM)	PO AUC (uM*h)	%F
Rat[a]	24 ± 8.0	4.2 ± 1.0	0.36 ± 0.3	2.3 ± 1.0	~9
Dog[b]	8.4 ± 2	7.7 ± 2.0	0.29 ± 0.02	1.7 ± 0.3	~35
Monkey[b]	5.2 ± 0.3	16 ± 4.0	0.1 ± 0.04	1.2 ± 0.4	~17

[a]5 mg/kg IV (3%DMA in 40% HPβCD; 30 mg/kg PO (0.4% HPMC in water))
[b]1 mg/kg IV (20% HPβCD; 2 mg/kg PO (10%T80/90% PEG400))

EBR was a substrate for human CYP3A4 only. Given that drug was eliminated unchanged in both rats and dogs suggesting other elimination pathways in addition to CYP3A4 metabolism, the potential for DDI as a victim for CYP3A4 inhibitors or inducers was also predicted to be low. EBR was shown to be a substrate for human OATP1B3.

7 Preclinical Safety Assessment Studies

EBR had no effect on hERG current up to the maximum tested concentration of 30 μM (400× to 1,300× the projected human C_{max} = 20–70 nM). When corrected for plasma protein binding in humans (~99%), this value was approximately 600,000×–5,600,000× the projected human C_{max} (Fu ~0.23–0.7 nM). Similarly, EBR had no effect on I_{Ks} and I_{Na} and minimal effect on I_{CaL} currents at 30 μM. EBR had no effect on heart rate or arterial blood in conscious rats at doses ≤40 mg/kg, and at doses up to 50 mg/kg, there were no test-article-related findings, thus establishing a no-observed-effect level (NOEL) at ≥50 mg/kg.

Potential hydrolysis products (both carboxylic acid and amine) from the parent structure were visually inspected for literature-based structural alerts for genotoxicity and found to be negative. EBR was tested for mutagenicity in a five-strain exploratory microbial mutagenesis (Ames) assay with and without S-9 up to 5,000 μg/plate and was found to be negative. As an antiviral compound, EBR was also tested for the induction of micronuclei in vitro in Chinese hamster ovary cells at 3 h after dosing with and without S9 and at 24 h after dosing without S9. The compound was negative up to 5 μM, and the top dose scored was limited by the precipitation of the test article. In addition, EBR was tested for micronucleus induction in rat bone marrow from a 4-day oral biomarker gene expression study at 1 day after the last treatment at 30 and 300 mg/kg/day for 4 days and found to be negative.

EBR was evaluated in an exploratory oral pharmacology study in dogs and an exploratory 7-day oral tolerability study in male rats at doses up to 750 mg/kg/day which corresponded to projected exposure multiples of 30–70× [AUC] and 40–120× [C_{max}]. There were no test-article-related findings; and the NOEL (and NOAEL) for this study was ≥750 mg/kg/day. EBR was also administered orally to Beagle dogs at doses up to 750 mg/kg. Assessments consisted of mortality, physical signs, and serum biochemistry evaluations which showed no adverse events nor any changes in serum biochemistry parameters.

In longer-term safety studies, no target organs of toxicity were identified, following oral EBR administration of up to 1,000 mg/kg/day, in toxicology studies in mice, rats, and dogs for up to 1, 6, and 9 months.

8 Synthesis

The first-generation synthesis of EBR proceeded in eight linear steps (twelve total steps) from commercially available materials with a 3% non-optimized yield from the longest linear sequence (Scheme 2). Thus, the C2' phenylindole intermediate **33a** was prepared by starting from 5-bromoacetophenone and *p*-bromophenylhydrazine using well-established two-step Fisher indole conditions. The indole NH group was cyclized onto the C2' phenolic group using standard alkylating conditions to give the racemic tetracyclic scaffold **33b** in good overall yield. The dibromide intermediate was subsequently converted into the corresponding pinacolboronate ester **33c** using standard procedures. Boronate ester **33c** was then coupled with two equivalents of the heterocyclic bromide **22b** in the presence of a catalytic amount of $Pd(dppf)Cl_2$ followed by workup, and deprotection of the Boc groups provided the desired compound **33d** in 57% yield. Amide coupling with *N*-methoxycarbonyl-L-valine afforded compound **33** as a mixture of diastereomers which were easily separated by SFC chromatography. EBR was the second diastereomer to elute and was determined to be the *S,S,S,S,S* diastereomer by single-compound X-ray analysis.

An enantioselective synthesis of the tetracyclic scaffold (**33k**) was developed by the Merck Process Chemistry team and featured a highly enantioselective asymmetric hydrogenation of an imine (**33g** → **33h**) and a directed stereochemical relay strategy that leveraged a dynamic diastereoselective condensation to produce the challenging hemiaminal stereocenter [11, 12]. The improved synthesis of EBR required only ten linear steps for completion in the longest linear sequence and proceeded in 30% overall yield without the need for chromatography (Scheme 3).

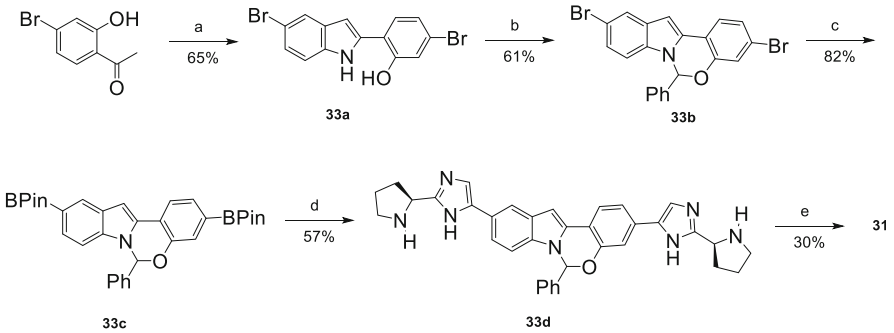

Scheme 2 Medicinal chemistry route for the synthesis of Elbasvir. (**a**) i. *p*-bromophenylhydrazine, AcOH, EtOH, reflux, ii. PPA, 110°C. (**b**) α,α-dibromotoluene, K_2CO_3, DMF, 100°C. (**c**) Bis (pinacolato)diboron, KOAc, $Pd(dppf)Cl_2$, dioxane, reflux. (**d**) i. 22b, Na_2CO_3, $Pd(dppf)Cl_2$, THF, water, reflux; ii. HCl, MeOH. (**e**) *N*-Moc-L-valine, BOP, DIPEA, DMF and then chiral SFC

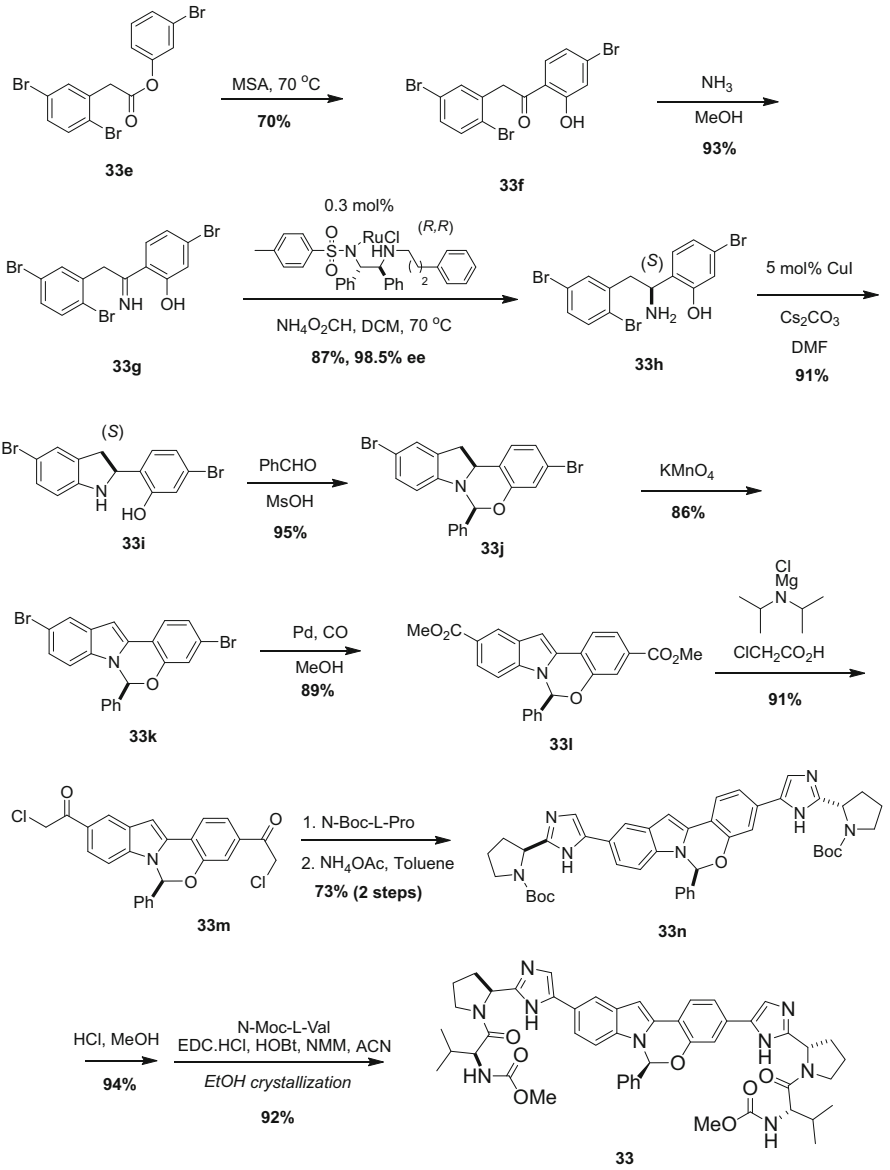

Scheme 3 Process chemistry route for the synthesis of elbasvir

9 Early Phase Clinical Trials

EBR was approved as a development candidate by Merck on December 9, 2010. In 2011, EBR was evaluated in healthy young male volunteers to assess the initial safety and plasma pharmacokinetics of single rising oral doses from 5 to 300 mg in healthy young male subjects. Proof of pharmacology targets were based on achieving exposures with a high likelihood of attaining proof of concept in a phase Ib study as judged by benchmarks set by BMS-790052. Using BMS-790052 PK and viral load data following 14 days of QD administration, the PK/PD relationship was assessed to determine the steady-state and Day 1 C_{24hr} targets that were likely to result in a 3 $\log_{10}$ viral load decline from baseline. The PK targets were adjusted for both potency against the GT1a virus and protein-binding differences between BMS-790052 and EBR using the EC_{90} values determined in 40% normal human serum. On this basis, the steady-state PK target for EBR was set at $C_{24hr,ss} \geq 3$ nM.

A summary of the mean plasma concentration-time profiles in healthy male subjects is presented in Fig. 4. Results from the study showed that the compound was rapidly absorbed, with a median T_{max} of 3.5–4.0 h for the 5–300 mg doses, and a

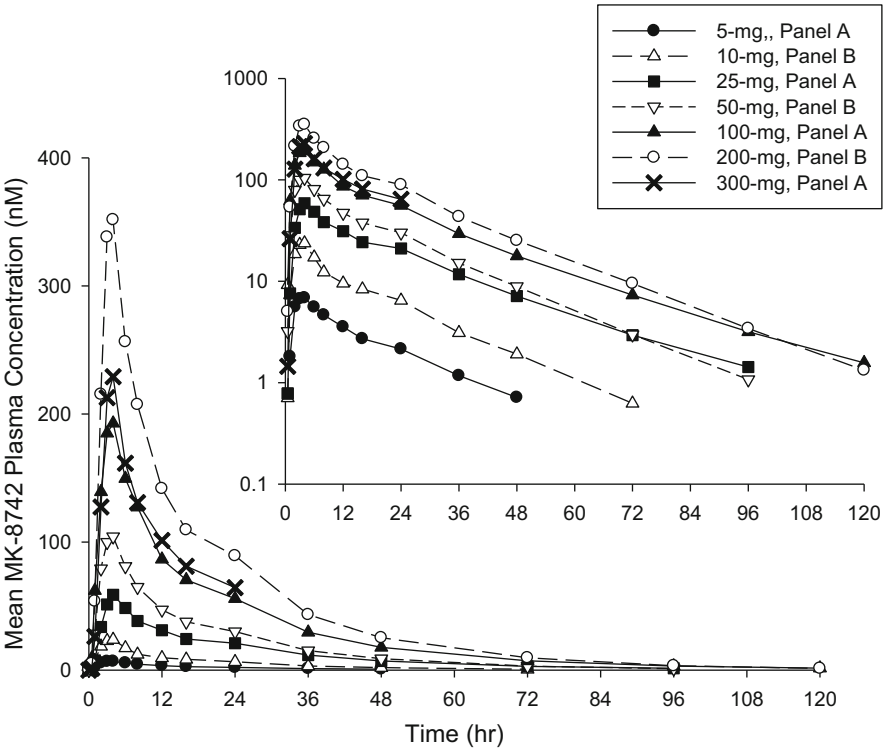

Fig. 4 Arithmetic mean plasma concentration profiles for EBR (EBR) following single oral 5–300 mg doses of EBR ($N = 6$/panel, linear scale, inset = semi-log) (LLOQ = 0.283 nM)

mean time delay $\leq$0.5 h was observed in most subjects at all doses. Drug concentrations appeared to decline after T_{max} in a biphasic manner, with the second phase initiating at about 12 h post-dose across doses. The mean terminal half-life ($T_{1/2}$) was ~14.5–19.1 h across the dose range studied and was consistent with the human PK predicted half-life of 14 h based on allometric scaling of preclinical data.

In 2013 results from a phase 1b randomized double-blind, placebo-controlled, multiple-dose study in HCV GT1-infected patients (PN002, "A Multiple Dose Study to Evaluate the Safety, Pharmacokinetics and Pharmacodynamics of EBR in Hepatitis C-Infected Males") demonstrated efficacy after once-daily dosing at a range of doses between 5 and 100 mg. Following once-daily dosing of 50 mg of EBR QD $\times$ 5 days, the mean maximum reduction in HCV viral load in GT1b patients was -5.1 (0.30) $\log_{10}$ IU/mL. The pattern of initial viral load decline was similar to that of the 10 mg panel. Following cessation of 50 mg dosing on day 5, the viral load remained suppressed at day 13 with a mean reduction of -4.75 $\log_{10}$ IU/mL followed by a rebound to -1.7 $\log_{10}$ IU/mL of VL decline by 3 weeks post-dose and a return to approximately baseline by month 2 after dosing (Fig. 5).

In the phase 2 dose-ranging study in combination with the protease inhibitor MK-5172 (Grazoprevir, GZR), 50 mg QD of EBR provided efficacy similar to that obtained with 20 mg QD EBR in a 12-week therapy with 100 mg QD GZR and

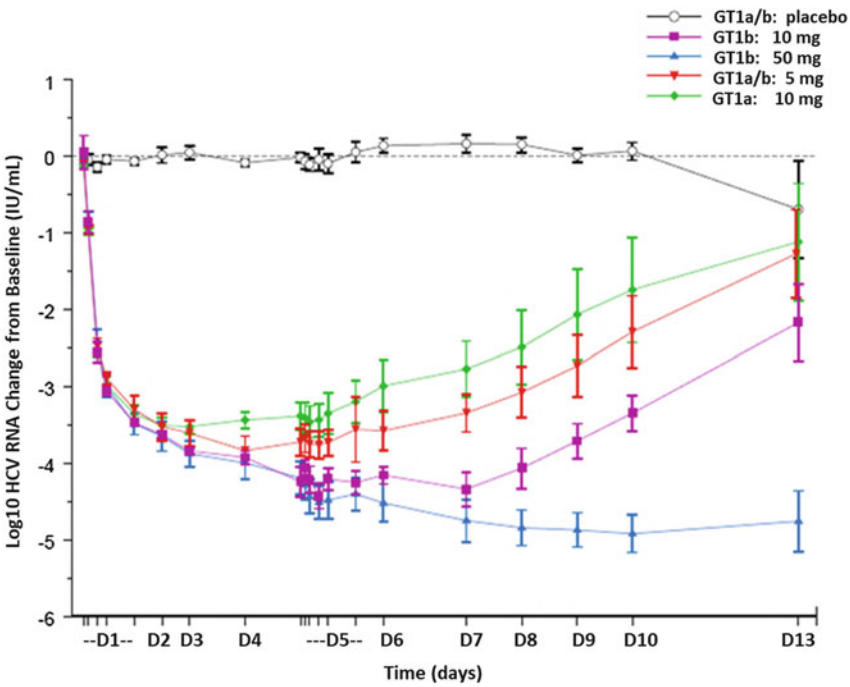

Fig. 5 Profiles of the change from baseline in $\log_{10}$ HCV RNA for GT1 HCV-infected male patients after receiving multiple once-daily doses of elbasvir/placebo for 5 days. *HCV RNA BLOQ is 25 IU/mL and that the BLOQ samples were imputed to 0.5 $\times$ 25 IU/mL

ribavirin, with SVR12 rates of 100% (22/22) and >95% (23/24) observed at 20 and 50 mg, respectively. While SVR12 response rates were similar between 20 mg QD and 50 mg QD EBR, the higher dose was selected for further evaluation in combination with 100 mg QD GZR.

10 Summary

On January 28, 2016, the US Food and Drug Administration approved Zepatier™ (elbasvir and grazoprevir) for the treatment of adult patients with chronic hepatitis C virus GT1 or GT4 infection. The discovery of elbasvir was the result of an intensive research effort that combined components from both internal and literature compounds that first led to a series of benzofuran-based NS5A structures which exhibited good potency versus genotype 1b. A detailed medicinal chemistry effort powered by a team of chemists from WuXi AppTec was then undertaken and included the exploration of various amide bond isosteres. This work ultimately led to the incorporation of two imidazole subunits and afforded compounds with sub-nanomolar EC_{50} values against genotypes 1a and 2a. Further optimization of this series using an expanded panel of HCV genotypes and clinically relevant NS5A-resistant mutant strains led to the discovery of the early lead compound MK-4882 which showed efficacy in a nonhuman primate model at a moderate dose. Viral breakthrough with the genotype 1a-infected chimpanzee, however, focused attention on developing analogues that were more potent against resistant variants while maintaining or improving the broad genotype profile. Strategic incorporation of a cyclic constraint and further lead optimization efforts led to the discovery of EBR.

Compliance with Ethical Standards

Conflict of Interest The author declares that he has no conflict of interest.

Ethical Approval All applicable international, national, and/or institutional guidelines for the care and use of animals were followed. All procedures performed in studies involving human participants were in accordance with the ethical standards of the institutional and/or national research committee and with the 1964 Helsinki declaration and its later amendments or comparable ethical standards.

Informed Consent Informed consent was obtained from all individual participants included in the study.

References

1. Gao M, Nettles RE, Belema M, Snyder LB, Nguyen VN, Fridell RA, Serrano-Wu MH, Langley DR, Sun J-H, O'Boyle DR, Lemm JA, Wang C, Knipe JO, Chien C, Colonno RJ, Grasela DM, Meanwell NA, Hamann LG (2010) Chemical genetics strategy identifies an HCV NS5A inhibitor with a potent clinical effect. Nature 465:96–100
2. Conte I, Giuliano C, Ercolani C, Narjes F, Koch U, Rowley M, Altamura S, De Francesco R, Neddermann P, Migliaccio G, Stansfield I (2009) Synthesis and SAR of piperazinyl-N-

phenylbenzamides as inhibitors of hepatitis C virus RNA replication in cell culture. Bioorg Med Chem Lett 19:1779–1783
3. Serrano-Wu M, Belema M, Snyder LB, Meanwell NA, St Laurent DR, Kakarla R, Nguyen VN, Qiu Y, Yang X, Leet JE, Gao M, O'Boyle DR, Lemm JA, Yang F, Bristol-Meyers Squibb. Inhibitors of HCV replication. US patent application US20060276511
4. Lemm JA, Leet DJE, O'Boyle DR, Romine JL, Huang XS, Schroeder DR, Alberts J, Cantone JL, Sun J-H, Nower PT, Martin SW, Serrano-Wu MH, Meanwell NA, Snyder LB, Gao M (2011) Discovery of potent hepatitis C virus inhibitors with dimeric structures. Antimicrob Agents Chemother 55:3795–3802
5. Romine JL, Laurent DRS, Leet JE, Martin SW, Serrano-Wu MH, Yang F, Gao M, O'Boyle DR, Lemm JA, Sun J-H, Nower PT, Huang X, Deshpande MS, Meanwell NA, Snyder LB (2011) Inhibitors of HCV NS5A: from iminothiazolidinones to symmetrical stilbenes. ACS Med Chem Lett 2:224–229
6. Lawitz EJ, Gruener D, Hill JM, Marbury T, Moorehead L, Mathias A, Cheng G, Link JO, Wong KA, Mo H, McHutchinson JG, Brainard DM (2012) A phase 1, randomized, placebo-controlled, 3-day, dose-ranging study of GS-5885, an NS5A inhibitor, in patients with genotype 1 hepatitis C. J Hepatol 57:24–31
7. Lemm JA, O'Boyle DR, Liu M, Nower PT, Colonno R, Deshpande MS, Snyder LB, Martin SW, St Laurent DR, Serrano-Wu MH, Romine JL, Meanwell NA, Gao M (2010) Identification of hepatitis C virus NS5A inhibitors. J Virol 84:482–491
8. Yu W, Coburn CA, Nair AG, Wong M, Tong L, Dwyer MP, Hu B, Zhong B, Hao J, Yang D, Selyutin O, Jiang Y, Rosenblum SB, Kim SH, Lavey BJ, Zhou G, Rizvi R, Shankar BB, Zeng Q, Chen L, Agrawal S, Carr D, Rokosz L, Liu R, Curry S, McMonagle P, Ingravallo P, Lahser F, Asante-Appiah E, Nomeir A, Kozlowski JA (2016) Alkyl substituted aminal derivatives of HCV NS5A inhibitor MK-8742. Bioorg Med Chem Lett 26:3800–3805
9. Yu W, Coburn CA, Nair AG, Wong M, Rosenblum SB, Zhou G, Dwyer MP, Tong L, Hu B, Zhong B, Hao J, Ji T, Zan S, Kim SH, Zeng Q, Selyutin O, Chen L, Masse F, Agrawal S, Liu R, Xia E, Zhai Y, Curry S, McMonagle P, Ingravallo P, Asante-Appiah E, Lin M, Kozlowski JA (2016) Aryl or heteroaryl substituted aminal derivatives of HCV NS5A inhibitor MK-8742. Bioorg Med Chem Lett 26:3414–3420
10. Scheel TKH, Gottwein JM, Mikkelsen LS, Jensen TB, Bukh J (2011) Recombinant HCV variants with NS5A from genotypes 1-7 have different sensitivities to an NS5A inhibitor but not interferon-α. Gastroenterology 140:1032–1042
11. Li H, Chen C-y, Nguyen H, Cohen R, Maligres PE, Yasuda N, Mangion I, Zavialov I, Reibarkh M, Chung JYL (2014) Asymmetric synthesis of cyclic indole aminals via 1,3-stereoinduction. J Org Chem 79(18):8533–8540
12. Mangion IK, Chen C-y, Li H, Maligres P, Chen Y, Christensen M, Cohen R, Jeon I, Klapars A, Krska S, Nguyen H, Reamer RA, Sherry BD, Zavialov I (2014) Enantioselective synthesis of an HCV NS5a antagonist. Org Lett 16:2310–2313